Rectangular dielectric rod at microwave frequencies—Part II. Radiation characteristics

T. K. SEN* AND R. CHATTERJEE
Department of Electrical Communication Engineering, Indian Institute of Science, Bangalore 560012

Received on December 24, 1977

Abstract

In this paper the radiation pattern of a rectangular dielectric rod excited by a metal waveguide is theoretically derived from the two-aperture theory as well as by surface integration of the fields over the entire rod applying Love–Schelkunoff's Equivalence Principle. The theoretical results are compared with the observed patterns.

Key words: Dielectric rod, microwave frequencies, radiation characteristics

1. Introduction

Two approaches which are in frequent use in determining the radiation pattern of surface-waveguides are by (i) surface integration of fields over the entire dielectric rod and (ii) the two-aperture theory. In the former, the equivalent sheet currents are determined from the tangential components of electric and magnetic fields over the surface of the rod using Love–Schelkunoff's equivalence theorem[1], and from the sheet currents the radiation field can be found out from the general radiation formula[2]. The second approach differs from the first in treating the surface-waveguide as a transmission line and assuming that radiation takes place whenever there is a discontinuity along the guide. For most of the cases these discontinuities are the feed end and free end of the dielectric rod.

In this paper we emphasize the two-aperture theory. The theoretical results obtained with the other method will be compared with that obtained by the two-aperture theory. Observed radiation patterns of different rods are also presented. The relative strengths of radiation fields occurring from the feed end and the free end of the rod have been determined experimentally.

2. Two-aperture theory

(a) *Mechanism of radiation*

Fig. 1 shows the geometry of the dielectric rod excited by a metal waveguide carrying the dominant TE_{10} mode. The metal waveguide is terminated at the plane $Z = 0$

* Presently in the Dapartment of Physics, Delhi University, Delhi

and the dielectric waveguide of length L is plugged into the metal waveguide. Inside the metal waveguide the dielectric rod is pyramidally tapered to a point.

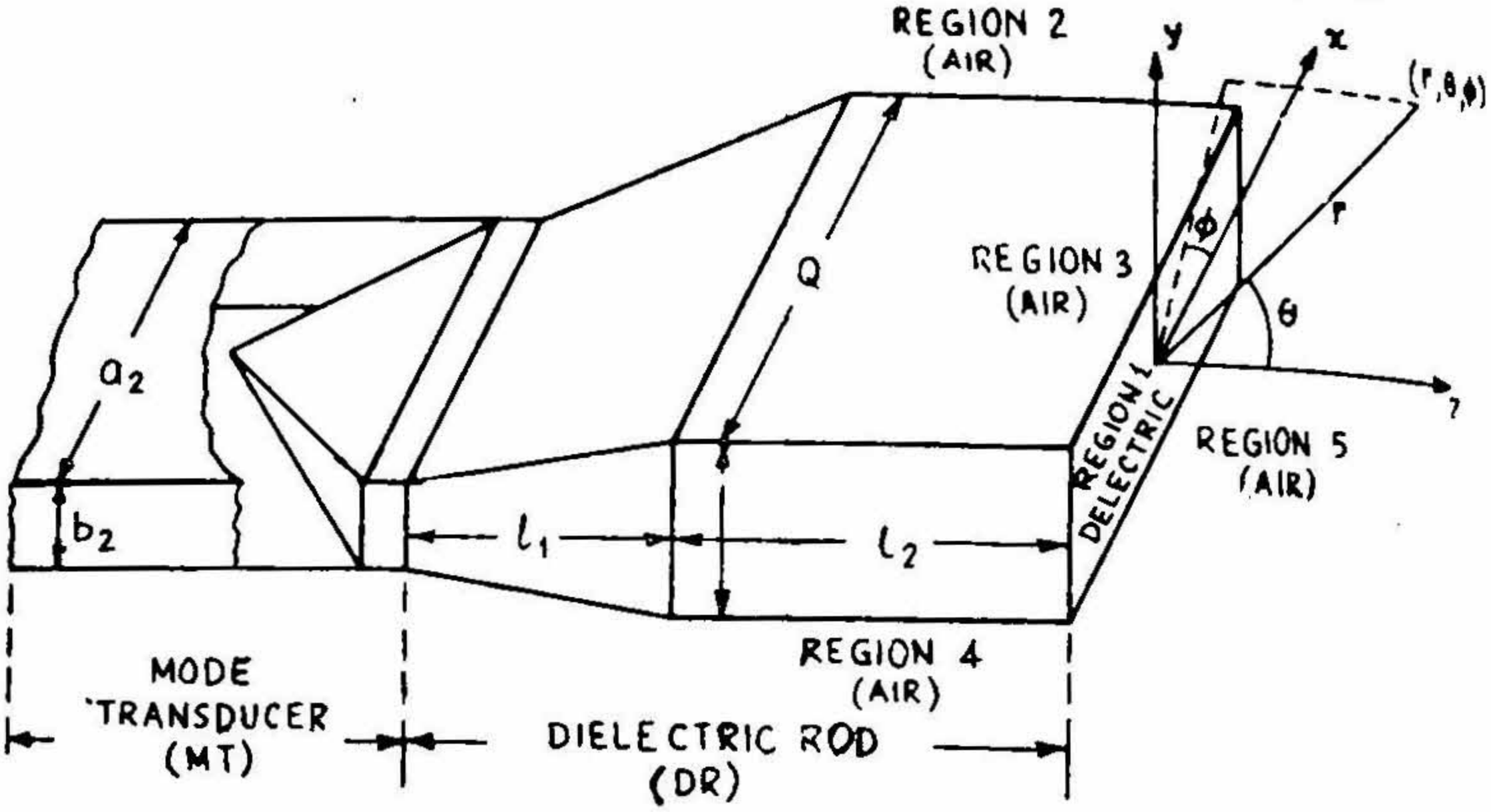

FIG. 1. Geometry of the mode transducer and the dielectric rod. MT = Mode transducer, DR = Dielectric rod.

If the dielectric material terminating the metal waveguide aperture were unbounded in both x and y directions, the fields in the region $z > 0$, which would have resulted due to the excitation of the metal waveguide, can be expressed as a continuous spectrum of plane waves. When the dielectric rod is of finite cross-section in the xy-plane a component plane wave undergoes multiple reflections from both the xz and yz interfaces of the dielectric rod. It is from the reflections of the various component plane waves as a function of the ray-direction the mechanism of radiation has to be understood as follows :

(i) When the dielectric constant ε_r of the material is greater than unity some of the rays undergo total internal reflections from both the xz and yz interfaces. There will be no power flow across the xz and yz interfaces because the fields are evanescent along both y and x directions. These rays therefore sustain no reflection loss at the interfaces and propagate without loss when the dielectric material of the rod is lossless. These are termed surface-waves having a discrete spectrum depending on the cross-sectional dimensions of the rod. These waves will radiate only when a discontinuity is introduced at any point along the length of the rod which in our case is due to the sudden termination of the rod at $z = L$, and $z = 0$ where the dielectric rod is plugged into the rectangular metal waveguide.

(ii) Rays may undergo only partial reflections at both the interfaces. At each reflection a portion of the energy leaks out from the surface of the rod and contri-

butes to the far-zone fields and the resultant fields are due to the superposition of the transmitted rays as a result of multiple reflections.

(iii) There will be two classes of rays which undergo total internal reflections either at the yz or at xz planes but not at both. These rays will also exert influence on the far-zone fields.

The rays classified in (ii) and (iii) will decay away along the z-axis because of leakage from the interface. These transmitted rays are a consequence of the feed end discontinuity of the rod and hence the radiation fields of these rays are called the radiation from the junction of the dielectric rod and the feeder.

We now proceed to find out individually the free end and the feed end radiation patterns. The resultant radiation pattern will be obtained by the superposition of these fields.

(*b*) *Feed end radiation*

The rectangular metal waveguide is excited in the TE_{10} mode. The electric and magnetic fields tangential to the aperture are given by

$$E_y = -\frac{w\mu_0}{\beta} \cos\ (\pi x/a_2) \tag{1}$$

$$H_x = \cos\ (\pi x/a_2) \tag{2}$$

The junction radiation field has been derived in a companion paper [Part I, Ref. 3]. The resultant junction radiation field in the $\phi = 0°$ plane obtained from equations (41) and (42) of Part I is given by

$$\begin{aligned} H_{\phi\,\text{junction}} = -\frac{2\pi jk_0 \cos\theta}{4\pi^2 r} \Bigg\{ & \frac{2A \exp\left[j(p-k_x)\,a/2\right]}{b\,(1-R_x^2)} \\ & \times (1+\rho_x)\frac{p}{k_x} T_m(k_x,\ \beta_y) \frac{\sin\,(\beta_y b/2)}{\beta_y} + \frac{\cos\,(\beta_x a/2)}{a + 2/\alpha_x} \\ & \times T_M(\beta_x, 0)\left[\frac{\exp\,(jpa/2)}{\alpha_x - jp} + \frac{\exp\,(-jp\,a/2)}{\alpha_x + jp}\right] \\ & + \frac{2A\cos\,(\beta_y b/2)\,T_M(k_x, \beta_y)}{b\alpha_y\,(1-R_x^2)} - \frac{p}{k_x}\frac{1+\rho_x}{1-R_x^2} T_M(k_x, 0). \\ & \times \exp\left[j(p-k_x)\,a/2\right] \Bigg\} \exp\ (-jk_0 r) \end{aligned} \tag{3}$$

where

$$A = \left[1 + 2\varepsilon_r (k_1^2 - k_0^2)\left\{\alpha_y b\,(\beta_y^2 + \varepsilon_r^2 \alpha_y^2)\right\}^{-1}\right]^{-1} \tag{4}$$

The summations over β_x and β_y are understood.

(c) *Free-end radiation*

The magnetic fields of the E^y modes[4] of the rectangular dielectric rod at the free-end of the rod at $Z = L$ in the regions 1, 2, 4, 3 and 5 are given by

$$H_{x1} = -A_1\omega\varepsilon_0\varepsilon_r\beta_z \cos(\beta_x x)\cos(\beta_y y)\exp(-j\beta_z L) \tag{5}$$

$$Hx_4^2 = -A_2\omega\varepsilon_0\beta_z \exp(T\alpha_x x)\cos(\beta_y y)\exp(-j\beta_z L) \tag{6}$$

$$Hx_5^3 = -A_3\omega\varepsilon_0\beta_z \cos(\beta_x x)\exp(T\alpha_y y)\exp(-j\beta_z L) \tag{7}$$

The angular spectrum of plane waves in region 1 is given by

$$F_{D1}(k_x, k_y) = \int_{x=-a/2}^{a/2}\int_{y=-b/2}^{b/2} H_{x1}\exp[j(k_x x + k_y y + k_{z0}L)]\,dxdy$$

or

$$F_{D1}(k_x, k_y) = -A_1\omega\varepsilon_0\varepsilon_r\beta_z \exp[j(k_{z0} - \beta_z)L]\frac{ab}{4}\cdot$$

$$\times\left(\frac{\sin P}{P} + \frac{\sin Q}{Q}\right)\left(\frac{\sin R}{R} + \frac{\sin S}{S}\right) \tag{8}$$

Similarly in region 2,

$$F_{D2}(k_x, k_y) + F_{D4}(k_x, k_y)$$

$$= \exp(jk_{z0}L)\int_{y=-b/2}^{b/2}\left[\int_{a/2}^{\infty} H_{x2}\exp\{j(k_x x + k_y y)\}\,dx + \int_{-\infty}^{-a/2} H_{x4}\exp\{j(k_x x + k_y y)\}\,dx\right]dy$$

or

$$F_{D2}(k_x, k_y) + F_{D4}(k_x, k_y)$$

$$= -A_2\omega\varepsilon_0\beta_z\frac{ab}{4}\exp[-\alpha_x a/2 + j(k_{z0} - \beta_z)L]$$

$$\times\left[\frac{\exp(-jk_x a/2)}{P_1} + \frac{\exp(jk_x a/2)}{Q_1}\right]\left[\frac{\sin R}{R} + \frac{\sin S}{S}\right] \tag{9}$$

and in region 3,

$$F_{D3}(k_x, k_y) + F_{D5}(k_x, k_y)$$

$$= -A_3\omega\varepsilon_0\beta_z \exp[-\alpha_y b/2 + j(k_{z0} - \beta_z)L]\frac{ab}{4}$$

$$\times\left[\frac{\exp(-jk_y b/2)}{R_1} + \frac{\exp(jk_y b/2)}{S_1}\right]\left[\frac{\sin P}{P} + \frac{\sin Q}{Q}\right] \tag{10}$$

where

$$P = (\beta_x + \kappa_x)\, a/2$$

$$Q = (\beta_x - k_x)\, a/2$$

$$R = (\beta_y + k_y)\, b/2$$

$$S = (\beta_y - k_y)\ \ b/2$$

$$P_1 = (\alpha_x + jk_x)\, a/2$$

$$Q_1 = (a_x - jk_x)\, a/2$$

$$R_1 = (\alpha_y + jk_y)\, b/2$$

$$S_1 = (\alpha_y - jk_y)\, b/2$$

$$k_{z0} = k_0 \cos\ \theta \tag{11}$$

The fields at a large distance ($k_0 r \gg 1$) can be evaluated in the $\phi = 0°$ plane ($k_y = 0$ by the method of stationary phase and are given by

$$H_{x\ \text{free-end}} = \frac{2\pi jk_0 \cos\theta}{4\pi^2 r} \exp\ (-jk_0 r)\, [T_{D1}\,(k_x, 0) + T_{D2}\,(k_x, 0) + T_{D3}\,(k_x, 0)] \tag{12}$$

Where $T_{D1}\ (k_x, 0)$ to $T_{D3}\,(k_x, 0)$ are determined from the corresponding expression of $F_D(k_x, 0)$ and are given by [eqn. 11, Part I]

$$T_{D1}\,(k_x,\ 0) = (1 - R_{D1})\, F_{D1}\,(k_x,\ 0)$$

$$T_{D2}\,(k_x,\ 0) = (1 - R_{D2})\, [F_{D2}\,(k_x, 0) + F_{D4}\,(k_x,\ 0)] \tag{13}$$

$$T_{D3}\,(k_x,\ 0) = (1 - R_{D3})\, [F_{D3}\,(k_x, 0) + F_{D5}\,(k_x\ \ 0)]$$

Where the R_D's, the reflection coefficients at the free-end of the rod in different regions can be derived in an exactly similar manner to equation (10), Part I and are given by

$$R_{D1} = [\varepsilon_r \beta_x\,(k_0^2 - k_y^2) - k_{x0}\,(\beta_z^2 + \beta_z^2)]\, [\varepsilon_r \beta_x\,(k_0^2 - k_y^2) + k_{x0}\,(\beta_z^2 + \beta_z^2)]^{-1} \tag{14}$$

$$R_{D2} = [\beta_x\,(k_0^2 - k_y^2) - k_{x0}\,(\beta_z^2 - \alpha_x^2)]\, [\beta_x\,(k_0^2 - k_y^2) + k_{x0}\,(\beta_z^2 - \alpha_x^2)]^{-1} \tag{15}$$

$$R_{D3} = [\beta_z\,(k_0^2 - k_y^2) - k_{z0}\,(\beta_x^2 + \beta_x^2)]\, [\beta_z\,(k_0^2 - k_y^2) + k_{z0}\,(\beta_x^2 + \beta_x^2)]^{-1} \tag{16}$$

Inserting the expressions for the T_D's from equation (13) in equation (12) we obtain in $\phi = 0°$ plane (*i.e.*, $k_y = 0$)

$$\begin{aligned} H_{x\ \text{free-end}} = \frac{2\pi jk_0 \cos\theta}{4\pi^2 r} \exp\ (-jk_0 r)\, &[(1 - R_{D1})\, F_{D1}\,(k_x,\ 0) \\ &+ (1 - R_{D2})\, \{F_{D2}\,(k_x, 0) + F_{D4}\,(k_x, 0)\} + (1 - R_{D3}) \\ &\times \{F_{D3}\,(k_x, 0) + F_{D5}\,k_x, (0)]\} \end{aligned} \tag{17}$$

The resultant radiation pattern is given by the superposition of the fields obtained from equations (3) and (17).

The constants A_1 to A_3 in equations (5) to (7) are the excitation constants and can be determined from the residue term of the integrals of equations (13), (18) and (19) respectively of Part I and are given by

$$A_1 = \frac{4\,(D_X'\,D_Y')^{-1}}{\omega\varepsilon_0\varepsilon_r\beta_z}\,T_M\,(\beta_x, \beta_y) \tag{18}$$

$$A_2 = \frac{4\,(D_X'\,D_Y')^{-1}}{\omega\varepsilon_0\beta_z}\cos\,(\beta_x a/2)\exp\,(\alpha_x a/2)\,T_M\,(\beta_x, \beta_y) \tag{19}$$

$$A_3 = \frac{4\,(D_X'\,D_Y')^{-1}}{\omega\varepsilon_0\beta_z}\cos\,(\beta_y b/2)\exp\,(\alpha_y b/2)\,T_M\,(\beta_x, \beta_y) \tag{20}$$

3. Radiation pattern by Schelkunoff's Equivalence Principle

Application of Love-Schelkunoff's equivalence principle to dielectric rod radiators is extensively described in literature[5] and will be briefly discussed.

The field components of the E^y modes are written as :

$$E_{x1} = A_1\beta_x\beta_y \sin\,(\beta_x x)\sin\,(\beta_y y)\exp\,(-j\beta_z z) \tag{21}$$

$$E_{y1} = A_1\,(\beta_x^2 + \beta_z^2)\cos\,(\beta_x x)\cos\,(\beta_y y)\exp\,(-j\beta_z z) \tag{22}$$

$$E_{z1} = -A_1\beta_y\beta_z \cos\,(\beta_x x)\sin\,(\beta_y y)\exp\,(-j\beta_z z) \tag{23}$$

$$H_{x1} = -A_1\omega\varepsilon_0\varepsilon_r\beta_z \cos\,(\beta_x x)\cos\,(\beta_y y)\exp\,(-j\beta_z z) \tag{24}$$

$$H_{z1} = -JA_1\omega\varepsilon_0\varepsilon_r\beta_x \sin\,(\beta_x x)\cos\,(\beta_y y)\exp\,(-j\beta_z z) \tag{25}$$

The closed surface of integration is shown in Fig. 2, the contributions due to only the following surfaces being significant.

(i) Free end : $-\frac{a}{2} < x < \frac{a}{2}$, $-\frac{b}{2} < y < \frac{b}{2}$, $z = 0$

(ii) Narrow walls : $x = -a/2$ and $a/2$, $-\frac{b}{2} < y < \frac{b}{2}$, $-L < z < 0$

(iii) Broad walls : $y = -b/2$ and $b/2$, $-a/2 < \times < a/2$, $-L < z < 0$

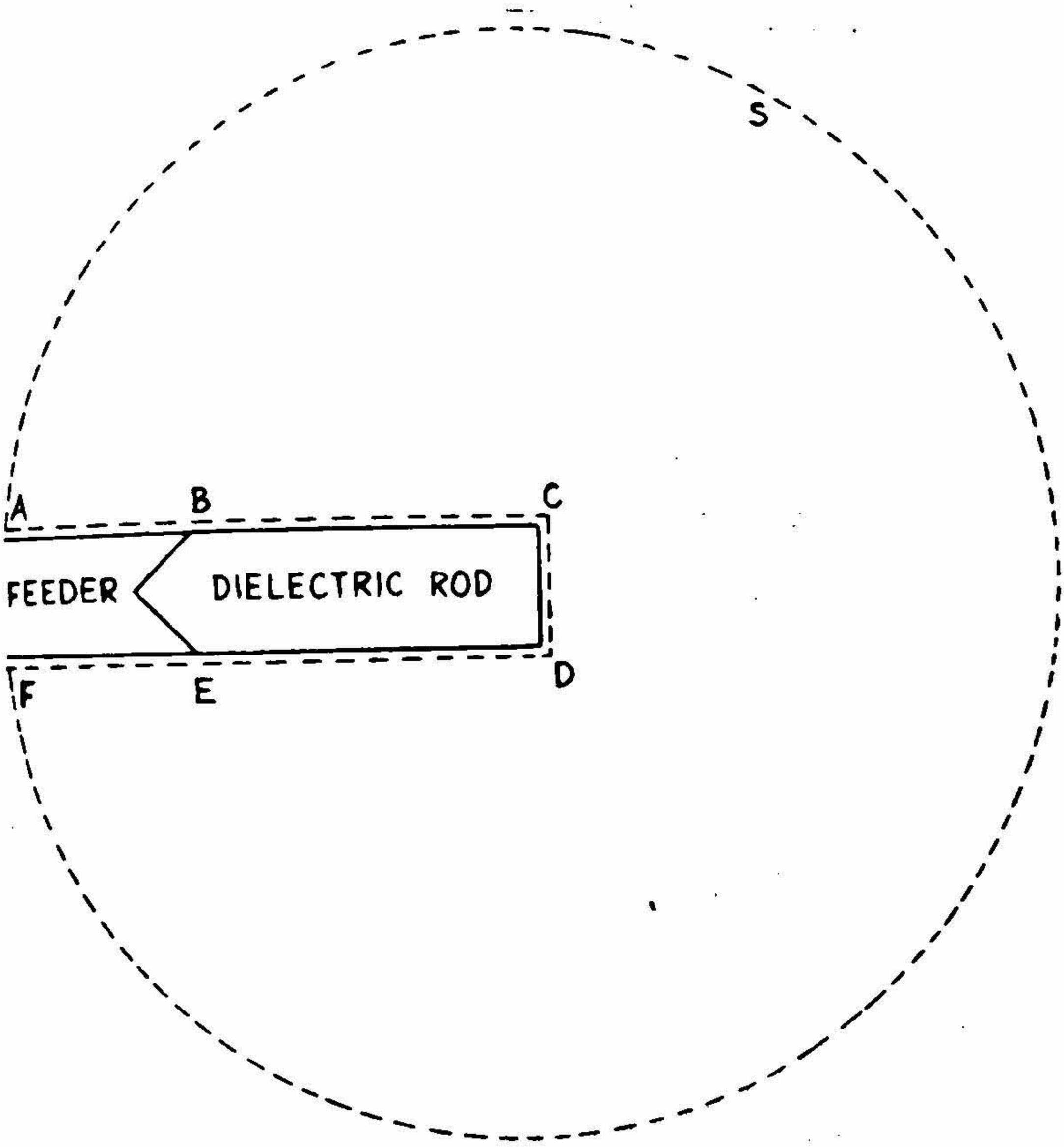

FIG. 2. Surface of integration.

At each surface the equivalent electric and magnetic sheet currents $\vec{J}$ and $\vec{K}$ are computed from the tangential components of the magnetic and electric fields ($\vec{H}$, $\vec{E}$) on the surface as follows :

$$\vec{J} = \vec{n} \times \vec{H} \tag{26}$$

$$\vec{K} = -\vec{n} \times \vec{E} \tag{27}$$

where $\vec{n}$ is the outward drawn normal at the surface.

The electric and magnetic radiation vectors ($\vec{N}$, $\vec{L}$) are computed as follows:

$$\vec{N} = \iint_S \vec{J} \exp\left[jk_0 (S_1 x + S_2 y + CZ)\right] ds \tag{28}$$

$$\vec{L} = \iint_S \vec{M} \exp\left[jk_0 (S_1 x + S_2 y + CZ)\right] ds \tag{29}$$

where

$$\begin{aligned} S_1 &= \sin\theta \cos\phi \\ S_2 &= \sin\theta \sin\phi \\ C &= \cos\theta \end{aligned} \tag{30}$$

S denotes the surface of integration and for the rectangular dielectric rod the integrations have to be carried out on five different surfaces mentioned earlier. The far-field is given[2] by

$$E_\phi = \frac{j \exp(-jk_0 r)}{2\lambda_0 r} \left[L_\theta - (\mu_0/\varepsilon_0)^{1/2} N_\phi\right] \tag{31}$$

Where L_θ and N_ϕ are the θ and ϕ components of $\vec{L}$ and $\vec{N}$ in spherical polar coordinates and λ_0 is the free-space wavelength.

Omitting the details of the evaluation, the field in $\phi = 0°$ plane ($E_\phi = E_y$ in $\phi = 0$, plane) is written as

$$\begin{aligned} E_y = \frac{J \exp(-jk_0 r)}{2\lambda_0 r} A_1 \Bigg[& (\beta_x^2 + \beta_z^2) \frac{ab}{2} \left(\frac{\sin P}{P} + \frac{\sin Q}{Q}\right) \frac{\sin R}{R} \\ & \times \left(\cos\theta + \frac{k_0 \varepsilon_r \beta_x}{\beta_x^2 + \beta_z^2}\right) + a\beta_y \sin(R)\, T \Bigg\{ \beta_x \cos\theta \left(\frac{\sin P}{P} + \frac{\sin Q}{Q}\right) \\ & - \beta_x \sin\theta \left(\frac{\sin P}{P} - \frac{\sin Q}{Q}\right) \Bigg\} - 2b \frac{\sin R}{R} T \left\{(\beta_x^2 + \beta_z^2) \cos(\beta_x a/2) \right. \\ & \left. \times \sin(k_0 s_1 a/2) \sin\theta - k_0 \varepsilon_r \beta_x \sin(\beta_x a/2) \cos(k_0 s_1 a/2)\right\} \Bigg] \end{aligned} \tag{32}$$

where

$$T = \left[\exp\left\{-j (k_0 c - \beta_x) L\right\} - 1\right] (k_0 c - \beta_x)^{-1} \tag{33}$$

and P, Q, R, S given by equations (38), (43) and (44) of Part I with $k_x = k_0 s_1$, $k_y = k_y = k_0 s_2 = 0$ in $\phi = 0°$ plane.

In equation (32) the first, second and the third terms are the contributions respectively from the free-end, broad walls and the narrow walls of the rod.

4. Numerical calculations and experimental results of radiation patterns

Radiation patterns calculated from the two-aperture theory and Love-Schelkunoff's equivalence principle are shown in Fig. 3 together with the experimental patterns for perspex ($\varepsilon_r = 2{\cdot}56$) rods of different dimensions.

It is to be noted that the length L of the rod appearing in the radiation patterns of either theory will be different from the physical length of the rod due to three reasons :

(i) There will be a change of phase because the mode on either side of the junction between the feeder and the dielectric rod have different configurations.

(ii) A change of phase will likewise occur at the free-end of the rod.

(iii) A portion of the dielectric rod outside the metal waveguide aperture has been tapered (Fig. 1) for gradual change of cross-sectional dimension of the rod.

No correction factor has been introduced for the cases (i) and (ii). For the tapered section an equivalent length has been obtained as follows :

Let l_1 be the axial length of the tapered section and l_2 be the length of the uniform rod. Over l_1, β_z will vary with z because of taper and the total phase shift over l_1 will be given by

$$\Delta\phi = \int_0^{l_1} \beta_z(z)\, dz \tag{34}$$

If β_s is the propagation constant of the uniform rod the equivalent length of the tapered section is given by

$$l_3 = \Delta\phi/\beta_s \tag{35}$$

Hence the length of the dielectric rod is given by

$$L = l_2 + l_3 \tag{36}$$

Turning now to the expression [Eqn. (3)] for the junction radiation pattern, it is worthwhile noting that the expression does not yield a null at $\theta = 0$ (*i.e.*, $p = 0$) because of the second and the third terms. In the case of surface-waveguides which can be represented as reactance surfaces, the application of impedance boundary condition necessarily yields a null along the interface in the zeroeth order evaluation of the feed radiation pattern by the method of steepest descent path. This is referred to as Karp-Karal lemma[6]. In the present case the appearance of a sharp dip in the experimental radiation patterns of some of the rods indicate that there is an appreciable amount of junction field along the interface of the rod (*i.e.*, between the rectangular rod and the free space) because the dips are the results of interference between the junction and the free-end radiation fields. Experimentally it has been observed by Zucker[7] that an appreciable amount of junction radiation occurs along the interface. Zucker's experi-

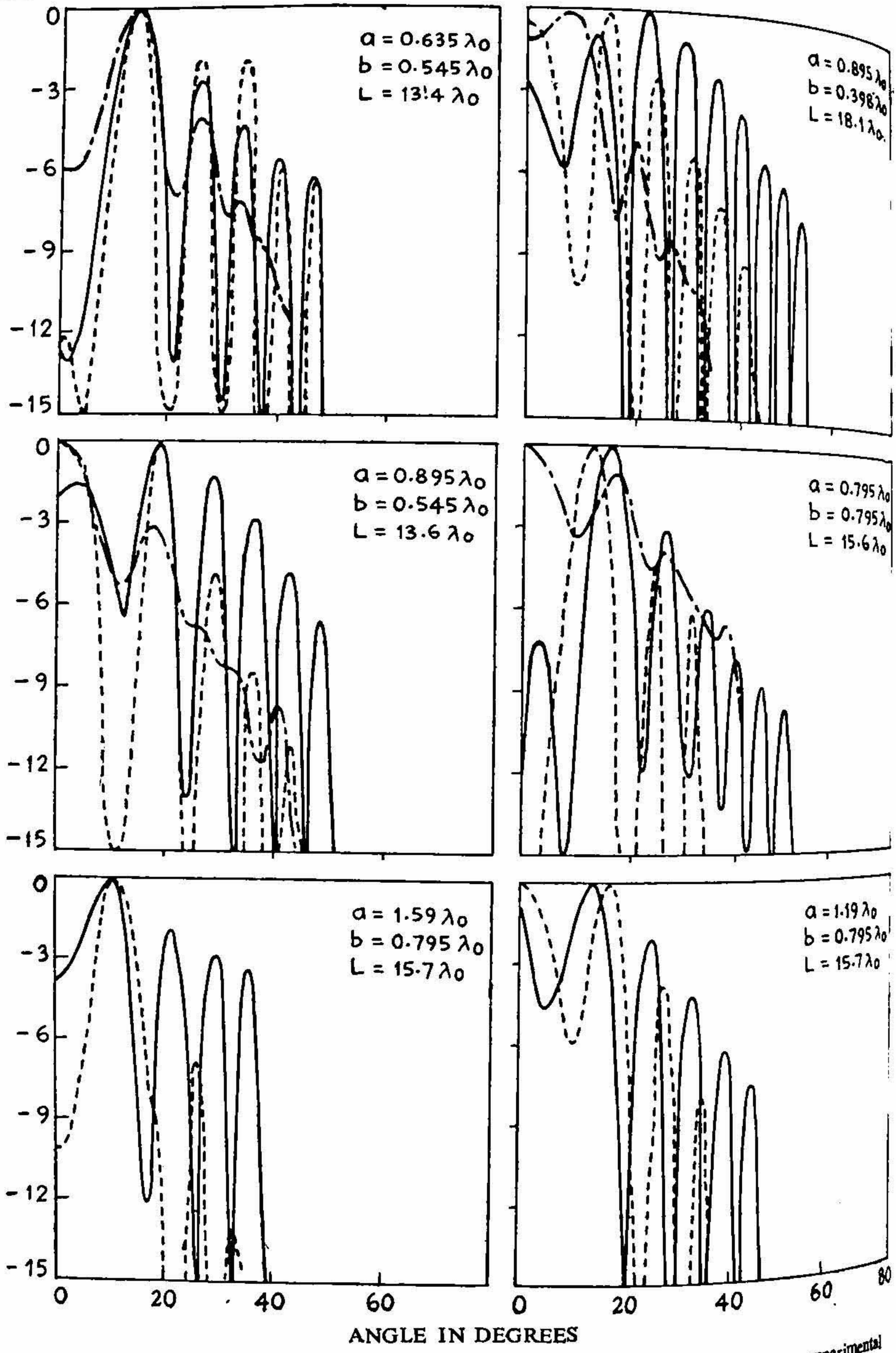

FIG. 3. Radiation patterns of rectangular dielectric rods ($\phi=0°$ plane $\lambda_0 = 3{\cdot}2$ cm) --- experimental

ment is repeated here to compare the strengths of the junction radiation fields with the free-end radiation fields for some of the rods.

5. Experimental determination of junction radiation fields compared to free-end radiation fields

In this method suggested by Zucker[7] the amplitude and the phase of the radiation fields are noted as functions of the length of the dielectric rod. The set-up is shown in Fig. 4. For measurement of phase, the received wave is compared with the reference wave in a slotted line by noting the position of the minimum. For amplitude measurements the reference wave is withdrawn from the other end of the slotted line and a matched load is connected to that end of the slotted line. If the crystal obeys a square

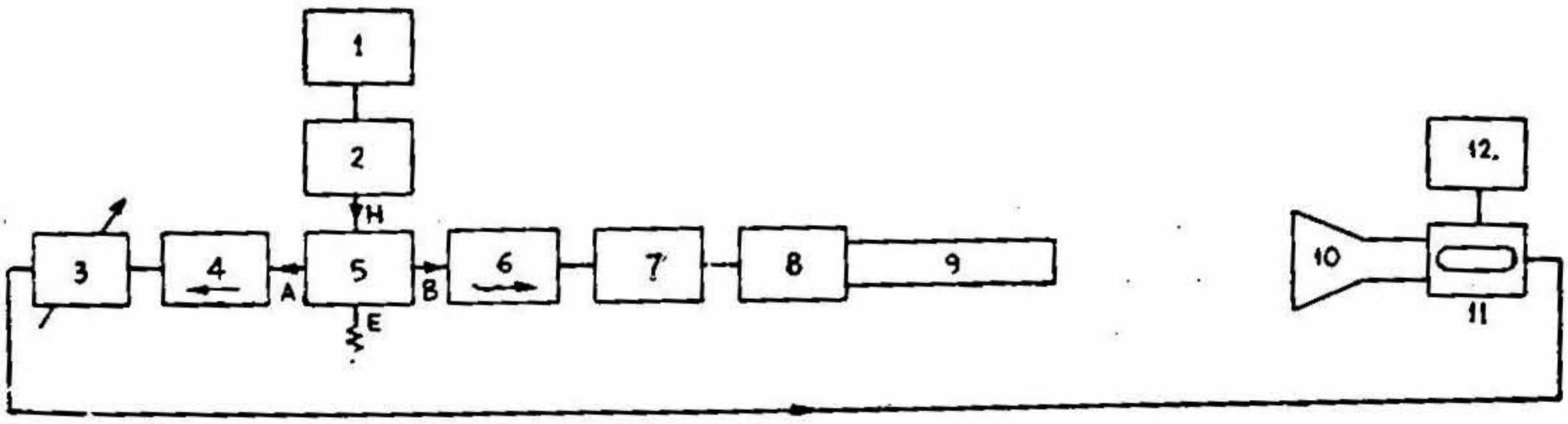

FIG. 4. Experimental set-up for the resolution of the surface-wave antenna patterns. (1) Power supply and square wave modulator, (2) Klystron 723 A/B. (3) Variable attenuator, (4) Isolator, (5) Hybrid tee, (6) Isolator, (7) Tuner, (8) Mode Transducer, (9) Dielectric rod, (10) Electromagnetic Horn, (11) Slotted section, (12) Detector and tuned amplifier.

law response the square root of the output meter indication is proportional to the amplitude of the received wave. The measurements are made for different lengths of the rod (by reducing the length of the rod by small steps). The complex points lie on a circle[7] whose centre is displaced from the centre of the polar plot by the amount proportional to the junction radiation field and the radius of the circle is proportional to the free-end radiation field.

The procedure can be repeated at all angles of observation so that the radiation patterns of the junction and of the free-end can be determined. Owing to the labour involved we have measured the relative strengths at $\theta = 0°$ only and the polar plot is shown for one rod (Fig. 5), while Table I shows the comparison of theoretical and experimental values for some of the rods at $\theta = 0°$.

For the lengths of the rod given in Table I, it is believed that the mutual coupling between the feed end and free-end apertures will be negligible. Hence the junction and the free-end radiation patterns will be independent of the lengths of the rods. It is also known that the strength of the quasi-near field which comes out of the first order term from the asymptotic evaluation of the branch-cut integral will be small at the termination of the rods when the lengths of the rods are large (*e.g.*, Table I) and hence the contri-

Table I

Relative strengths of the feed end and terminal radiation fields at $\lambda_0 = 3{\cdot}2$ cms.

a/λ_0	b/λ_0	L/λ_0	$\frac{E_{\text{junction}}}{E_{\text{free-end}}} = \frac{F(0)}{T(0)}$ at $\theta = 0°$ (Fig. 5)	
			Theory	Experiment
0·635	0·545	12·4	0·65	0·54
1·191	0·795	14·0	0·24	0·16
1·590	0·795	14·0	0·20	0·15

bution of the junction radiation at $\theta = 0°$ as observed experimentally cannot be due to the diffraction of the quasi-near field at the termination of the rod as has been discussed by Zucker in connection with his experiment[7]. The fact that Karp-Karal lemma is not satisfied [Sec. 4] is related to multi-interface structure studied in this paper. The theoretical values of the strengths of the junction radiation relative to that of the free-end radiation are higher than the experimental values, probably due to the fact that the tapered section of the rod outside the feeder provides better match (*i.e.*, higher launching efficiency) than that is assumed in the theory. The present theory also neglects any diffraction of the junction radiation fields at the termination of the rod.

6. Gain

The power gain of the antenna is defined by

$$G = \frac{\text{Maximum radiation intensity } U_M}{\text{(Maximum radiation intensity of a reference antenna with the same power input)}} \tag{37}$$

If P is the power input to the test antenna and U_0 is the radiation intensity of a lossless isotropic antenna with the same power input P, the total power radiated over a hemisphere is

$$P = 2\pi U_0 \tag{38}$$

Hence

$$G = 2\pi U_M/P \tag{39}$$

Power input to the antenna is the total power carried by the surface wave and the junction radiation that is,

$$P = P_s + P_r$$

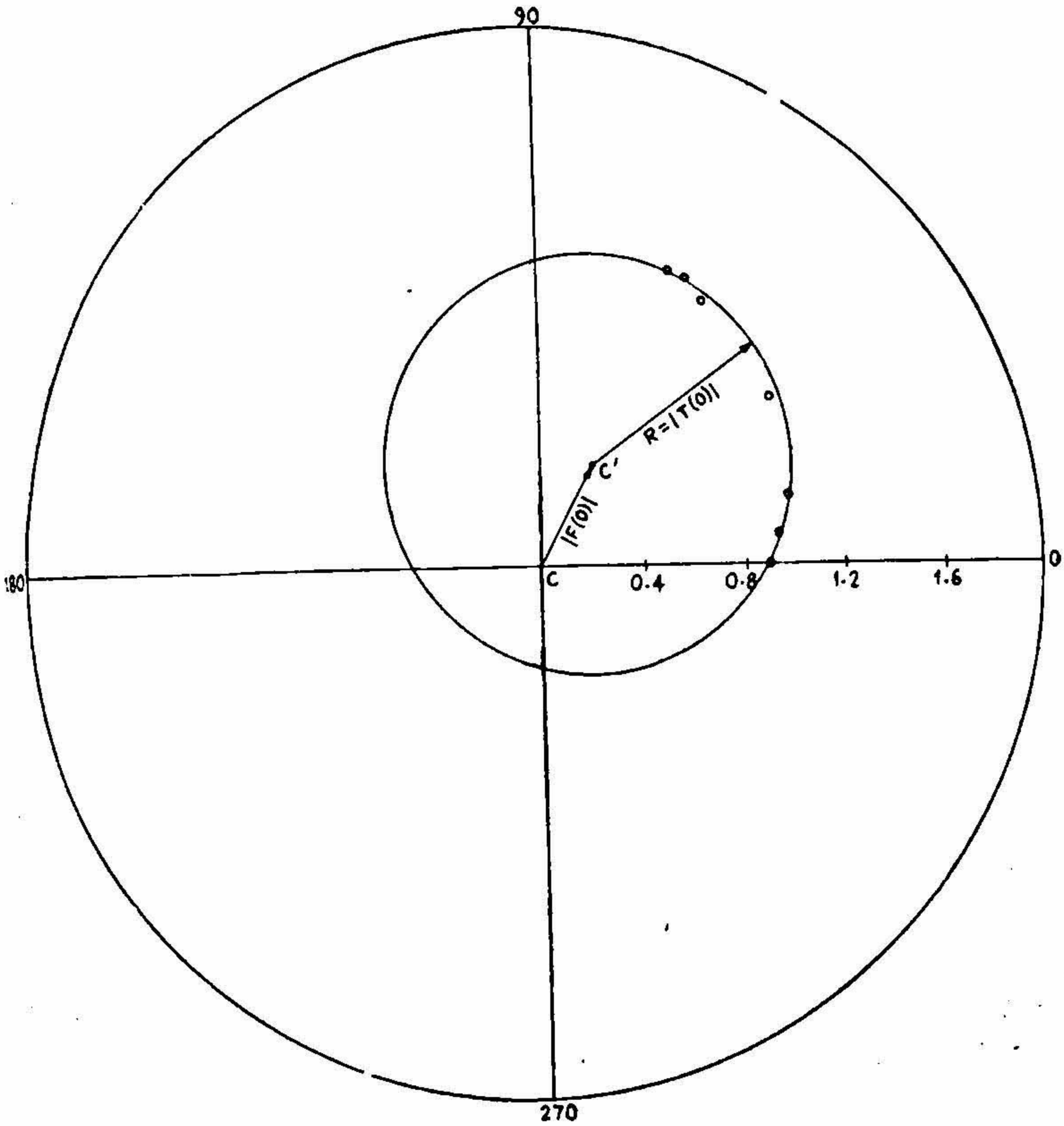

FIG. 5. Circle diagram for resolving surface-wave antenna patterns. $a = 0{\cdot}635\ \lambda_0$, $b = 0{\cdot}545\ \lambda_0$ $\lambda_0 = 3{\cdot}2$ cms.

$$\frac{|F(0)|}{|T(0)|} = \frac{CC'}{R} = 0{\cdot}54.$$

where P_θ and P_ϕ are given by equations (46) and (47) respectively of Part I. The maximum value of the radiation intensity of the test antenna has been found out theoretically from the expression of the resultant radiation pattern. To account for the modal attenuation of the rod the right hand side of equation (17) has been multiplied by the factor $\exp(-\alpha L)$ where α is the modal attenuation constant in nepers/cm of the mode under consideration. Theoretical gains are compared with the observed values in Table II.

Table II

Gain of the antennas ($0 = 3 \cdot 2$ cms).

a/λ_0	b/λ_0	L/λ_0	Gain *db*	
			Theory	Experiment
0·635	0·545	13·4	6·226	7·20
0·795	0·795	15·6	7·050	7·64
0·895	0·398	13·6	6·735	7·20
1·191	0·795	15·7	6·894	7·64
1·590	0·795	15·7	6·490	7·64

The discrepancies between the theoretical and the experimental values are ascribed to the facts that the effect of the tapered section of the rod provides better match than assumed in the theory and also that the energy carried away by the junction radiation field has been evaluated approximately [eqn. (51) Part I].

7. Discussions

It is observed from Fig. 3 that the experimental radiation patterns agree fairly well with those predicted by the two-aperture theory but the agreement with the patterns obtained by Schelkunoff's Equivalence Principle is not good. This disagreement is however not because of the method but due to the fact that the correct field distribution has not been used in the theory. It is evident that near the feed end of the rod, the fields on the surface of the rods at $x = \pm a/2$ and $y = \pm b/2$ are far from pure surface-wave fields and if the complex field distribution near the feed is accounted the pattern is likely to agree well. However, unfortunately, the determination of the complex field distributions near the feed is far more complicated than to account for the modification of the feed aperture radiation pattern in the presence of the rod as has been done for the two-aperture theory. It is to this extent that the two-aperture theory is superior to the other method. The derivation of radiation pattern by Schelkunoff's Equivalence Principle is approximate because it neglects any reflection of surface wave from the free-end of the rod which however is small enough to affect the nature of the radiation pattern appreciably.

It may appear that the application of field difference method for the derivation of the radiation pattern for the feed[8] is simpler than the method used here. But to find out the relative strength of the feed and free-end radiation patterns the knowledge of excitation constant is essential. The chopped surface-wave distribution which has

been assumed for deriving the excitation constant in the above reference applies only to the case of feed apertures which are large in dimensions to encompass the surface-wave field at least to e^{-1} of its value at the interface[6].

8. Acknowledgements

The authors wish to thank Professor S. Dhawan, Director, Indian Institute of Science for providing the necessary facilities for the above work and Professor S. K. Chatterjee, Hon. Retired Professor of the Institute for helpful discussions.

References

1. SCHELKUNOFF, S. A. — Some equivalence theorems of electro-magnetics and their application to radiation problems. *B.S.T.J.*, 1936, **15**, 92–112.

2. SCHELKUNOFF, S. A. — A general radiation formula. *Proc. I.R.E.*, 1939, **27**, 660–666.

3. SEN, T. K. AND CHATTERJEE, R. — Rectangular dielectric rod, Pt. I. Theoretical and experimental determination of launching efficiency. *Jour. I.I.Sc.*, 1978, **60**, (5), 193–210.

4. MARCATILI, E. A. J. — Dielectric rectangular waveguide and directional coupler for integrated optics. *B.S.T.J.*, 1969, **18**, 2071–2102.

5. KIELY, D. G. — *Dielectric Aerials*, 1953, Ch. III, pp. 59–76, Methuen and Co. Ltd., London.

6. COLLIN, R. E. AND ZUCKER, F. J. — *Antenna Theory*, 1969, Pt. 2, Ch. 21, McGraw-Hill.

7. ZUCKER, F. J. — Experimental resolution of surface-wave antenna radiation into feed and terminal patterns. *I.E.E.E. Trans.*, AP-18, 1970, 420–422.

8. JAMES, J. R. — Gain enhancement of microwave antennas by dielectric filled radomes. *Proc. I.E.E.*, 1975, **122**, 1353–1358.